RESEARCH ARTICLE

Editorial Process: Submission:11/03/2021 Acceptance:05/14/2022

A Descriptive Study of the Physical Direct Interaction between Adipose Tissue-Mesenchymal Stem Cells and Colo 205 Cells: Impact on Cancer Cells Stemness, and Intracellular Reactive Oxygen Species Levels

Nour Sharar[1,2], Amjad A Mahasneh[1]*, Djeda Belharazem[3], Nidaa Ababneh[2], Abdalla Awidi[2]

Abstract

Background: Mesenchymal stem cells (MSCs) are widely used in clinical research to treat a wild spectrum of diseases due to their homing ability to damaged tissues, self-renewal capacity, and differentiation ability into various types of cells. In this research, we are describing the physical direct interaction between AT-MSCs and colon cancer cells, its impact on the stemness of colon cancer cells, along with the levels of intracellular Reactive Oxygen Species (ROS) levels in both types of cells. **Methods:** Adipose-tissue mesenchymal stem cells (AT-MSCs) were characterized by the means of MSCs classical markers expression using flow cytometry, and multilineage differentiation through osteogenic and adipogenic differentiation. MSCs and colo205 cells were cocultured in monolayer and 3D techniques in a ratio of 1:3 for 72 hours without media exchange and compared to monocultured cells. The physical direct interaction of cells in adhered culture and spheroids formation in ULA plates was observed using a light-inverted microscope. MSCs classical markers and cancer stem cells (CSCs) associated surface proteins were quantified in MSCs and colo205 cells. Intracellular ROS level was measured in both cell types. Surface protein and intracellular ROS quantification were carried out using flow cytometry. **Results:** CRC cells (colo205 cells) utilized MSCs as a feeder layer to grow and generate spheroids. The interaction increased the percentage of CSCs in colo205 population which was attributed to the increased expression of CD133, and reduced the levels of intracellular ROS in MSCs. Results indicated that MSCs support the growth, spheriod formation, and the stemness of colon cancer cells, while reducing the levels of intracellular ROS in MSCs.

Keywords: Mesenchymal stem cells- adipose tissue- colorectal cancer- reactive oxygen species- cancer stem cells

Asian Pac J Cancer Prev, **23 (5)**, 1635-1646

Introduction

Colorectal cancer (CRC) is the fifth deadliest cancer in the world, accounting for 5.8% of all cancer deaths. Despite the advanced therapeutic approaches, CRC incidence rate has been steadily increasing worldwide (Rawla et al., 2019). In Jordan, CRC is the most common type of cancers among men and the second most common among women with a constant increasing rate among the population (Esr et al., 2018).

Colorectal cancer is composed of multiple populations of cells including malignant cells, cancer-associated fibroblasts (CAFs), endothelial cells, and mesenchymal stem cells (MSCs) (Chen et al., 2020; Tao et al., 2017; Powell et al., 2005). MSCs are multipotent adult stem cells with fibroblast-like morphology, self-renewal ability and high plasticity. Following the minimum criteria proposed by the International Society for Cellular Therapy (ISCT), In 2006, an isolated population of cells are classified as MSCs if they adhere to culture plates plastic surfaces, express classical surface markers (CD90, CD105, CD73 and CD44) and lack expression of hematopoietic stem cells markers (CD45, CD34, CD14 or CD11b, CD79a or CD19, and HLA-DR) , and differentiate into osteocytes, adipocytes and chondrocytes (Dominici et al., 2006). MSCs were suggested as a candidate for regenerative medicine due to their repairing ability, immunosuppressive properties and low immunogenicity (Lukomska et al., 2019; Joyce et al., 2010; Ritter et al., 2012). For that, MSCs are isolated from various adult tissue using a straightforward standard procedure, expanded in culture to obtain a huge number of cells which will be later utilized

*[1]Biotechnology and Genetic Engineering, Faculty of Science and Arts, Jordan University of Science and Technology, Irbid, Jordan. [2]Cell Therapy Center, The University of Jordan, Amman, Jordan. [3]University of Medicine Mannheim of the University of Heidelberg, Mannheim, Germany. *For Correspondence: amjada@just.edu.jo*

in the treatment of heart failure, neurodegenerative and autoimmune diseases (Joyce et al., 2010). MSCs can be isolated from various tissue sources such as: bone marrow, adipose tissue, amniotic fluid and umbilical cord. They were first isolated from bone marrow and utilized in cellular therapy, however adipose tissue obtained from lipoaspiration procedures provides a more convenient source of MSCs; due to the higher yield of primary cells that is provided by adipose tissue, and the collection of adipose tissue by a minimally invasive procedure (Alonso-goulart et al., 2017; Berebichez-Fridman and Montero-Olvera, 2018; Mohamed-Ahmed et al., 2018).

MSCs can be systemically applied into the body, most likely they will be trapped in the lung until their mobilization and migration to the sites of injuries are triggered by the inflammatory cytokines (Eggenhofer et al., 2014; Ullah et al., 2019). Following the same manner, MSCs home to and engraft primary and secondary tumor sites where they are believed to increase tumor progression through the induction of stemness, epithelial to mesenchymal transition (EMT) in tumor cells, along with angiogenesis, and the suppression of the host immune responses against abnormal cells (Kucerova et al., 2007; Cuiffo and Karnoub, 2012).

The use of MSCs in cellular therapy is in constant increase and their utilization in cancer-targeted therapy has been suggested and investigated without taking into consideration the effect of their behavior in the tumor microenvironment. In the past, studies have mainly focused on the interaction between cancer cells, neglecting their interaction with the stromal cells in the TME. Therefore, more studies need to investigate the interaction between stromal and cancer cells, and to evaluate the role and safety of MSCs in cellular therapy especially in the treating or targeting of cancer cells. The aim of this study was to investigate the physical direct interaction between AT-MSCs and colo205 cells, and evaluate its impact on colon cancer cells spheroid formation, stemness, and the level of intacelluar ROS in both types of cells.

Materials and Methods

AT-MSCs culture

AT-derived MSCs were obtained from the previously banked samples at the Cell Therapy Center (CTC)/ University of Jordan. These samples were collected from consented healthy females in the age range of (35-43). Donors recruitment and sample collection were approved by the University of Jordan IRB. Samples were received at passage one (P1) preserved in special cryopreservation media (Synth-a-Freeze Cryopreservation Medium, Gibco) at a density of 2-3 × 10^6 cells/mL. The culture of MSCs was conducted in alpha MEM medium with Earle's Salts (Euroclone) supplemented with 5% human platelet lysate (hPL) prepared in the CTC, 1% penicillin streptomycin, and 2 mM L-glutamine. Anticoagulant (Heparin-Sodium 5,000 I.U/mL) was added to media before adding hPL, it was used at a concentration of 3 I.U. This step was crucial to eliminate the gel formation in culture (Abuarqoub et al., 2019; Abuarqoub et al., 2015). Cells were cultured in an adherent plate at a seeding density of 4,000 cells/cm^2. Cells were subcultured whenever they became 80% confluence, until they reached P5.

Cancer Cell Culture

Colorectal cancer cells line (colo205) provided by the CTC cryopreserved at P9 was thawed and directly cultured at a seeding density of 1 × 10^6 cells/T75 in advanced DMEM medium (Gibco) supplemented with 10% heat inactivation (56°C-30min) FBS, 1% penicillin streptomycin, and 2 mM L-glutamine (Geng et al., 2014). When cells reached 70% confluence subculture was conducted. The collected cells from one T75 flask are distributed into four T75 flasks in a splitting ratio of 1:4. Cells usually took 3-4 days to reach 70% confluence.

Osteogenic and Adipogenic Differentiation of AT-MSCs

AT-MSCs were induced to differentiate into adipocytes or osteocytes when they reached P5 using osteogenic or adipogenic induction media prepared as reported in (Murphy et al., 2002). MSCs were cultured at seeding density of 4,000 cells/cm^2 in a 6-well plate using alpha-MEM supplemented with 5% hPL. When cells reached 70-80% confluence, culture media were replaced with differentiation media. Cells were maintained in culture for 3 weeks and media was replaced every 2-3 days. Morphological changes were monitored during the differentiation period using inverted microscopy. When the differentiation period was completed, culture media was aspirated leaving behind the generated monolayer of differentiated cells. Cells were washed twice with PBS before being fixed with 10% (v/v) formaldehyde in PBS for 20 minutes at room temperature. Then the fixative was removed and cells were washed with PBS twice. For adipocytes staining, an adequate volume of oil red O stain was added to cover the monolayer. After 30 minutes of incubation with the dye, cells were washed at least twice with PBS. For osteocytes staining, cells were washed with distilled water before adding an adequate volume of Alizarin red stain. The monolayer was left merged in the dye for 30 minutes before washing with distilled water. Stained, undifferentiated cells were used as a negative control. Cells were checked under an inverted microscope to visualize oil droplets in adipocytes or calcium deposit in osteocytes.

MSCs and Colo205 Coculture

A coculture between AT-MSCs and a metastatic cancer cell line (Colo205) was conducted in a monolayer. Colo205 cells were trypsinized and collected, washed with PBS twice to remove any residue of the FPS serum, then suspended in alpha-MEM supplemented with 5% hPL. MSCs were also collected in alpha-MEM. In Adherent Plate the coculture between the two type of cells was conducted at 1:3 ratio in an adherent plate, To achieve that, 40,000 MSCs were mixed with 120,000 colo205 cells per well in a 6-well plate. Cells were maintained in standard culture condition for 72 hours. as a control, 40,000 MSCs and 120,000 colo205 cells were cultured separately.

Flow cytometry

The spillover between the different fluorochrome

was corrected using Anti-Mouse Ig, κ/Negative Control (FBS) and Compensation Particles Set (BD Biosciences) as recommended by the manufacturers. In brief, The compensation control was prepared, a drop of anti-mouse Ig, κ beads were suspended in 100 μL staining buffer. A single antibody was added to the beads suspension and left at room Tm for 30 minutes. Cell washing buffer was then added to the beads then washed by centrifugation at 300 xg. Beads were suspended with PBS then a drop of the negative beads was added to each tube before acquired by the instrument. For surface markers staining, cells were harvested and suspended in 1X PBS then distributed to FACS tubes in which 5×10^5 cells were added per tube. Cells were stained with positive and negative antibody cocktails or their isotype controls with the concentration shown in (Tables 1, 2 and 3).

Intracellular ROS Assay

The relative ROS concentration was measured in cells using the fluorogenic reagent 2′,7′-dichlorofluorescin diacetate (DCFDA). After 72 hours of co-culture, cells from the three groups (MSCs cultured alone, colo205 cells cultured alone and 1:3 cocultured cells) were trypsinized and centrifuged at 350 xg for 6 minutes. Cells were resuspended in PBS and distributed into FACS tubes in an equal amount, then centrifuged to pellet the cells in the FACS tubes. After the removal of the supernatant, ROS staining reagent was added to cells and mixed. Cells were incubated for one hour in standard culture conditions. After incubation, cells were washed with PBS then re-suspended in FACS staining buffer before staining with 2μL of PE-anti CD44 antibody. CD44 was used as a differential marker to distinguish between MSCs and Colo205 and the level of intracellular ROS was measured in both populations. The fluorogenic DCF was excited using the blue laser (488 nm) and its emission (520 nm) was detected in the FL-1 channel. Fluorescence minus one (FMO) was used to eliminate overlapping between FL1 and FL2 channels. The median fluorescence intensity (MFI) of FL1 channel was used to indicate the relative intracellular ROS level.

FACS Instrument and Analysis

Sample acquisition was performed using BD FACS Canto II instrument. All data analysis was performed using 0.8 BD FACS DIVA software provided with the instrument. The analysis was performed using Median fluorescence intensity (MFI) or cell percentage (%). MFI was used to detect the overall change in the expression of the selected population, while the percentage indicated the change in the number of positive cells in that population.

Results

Characterization of AT-MSCs

The obtained MSCs samples were characterized by the mean of their surface markers expression, and differentiation into adipocytes and osteocytes. The expression of MSCs classical markers revealed a uniform high expression (> 90%) of MSCs positive markers (CD90, CD73, CD105, and CD44), and the negative expression (≤ 2% positive) of hematopoietic progenitor surface markers (CD34, CD11b, CD19, CD45, and HLA-DR) (Figure 1A). Their differentiation capacity was demonstrated through the morphological changes and histochemical staining (Figure 1B, 1C and 1D). These results correspond to the criteria that was proposed by the international society of cellular therapy to identify MSCs.

Physical direct interaction between MSCs and colo205 cells

In coculture, MSCs and colo205 cells were recognized from each other on the bases of the differences in their size and morphology; colo205 cells appeared smaller in size compared to MSCs with a round shape that is distinguishable from the flattened, spindle-like-shape morphology of MSCs. Colo205 cells adhered to the MSCs monolayer instead of the surface of the flask. After 72 hours of coculture, no morphological changes were observed in MSCs or in colo205 cells and both types of cells looked healthy.

Spheroid formation of colo205 cells cocultured with MSCs

The formation ability of multicellular spheroids in MSCs and colo205 cells was tested in U-bottom, 96 ultra-low adherent well plate, separately. MSCs formed a single multicellular spheroid in every well of the plate within 24 hours of culture. The generated spheroids were round in shape with a defined edges and a compact

Table 1. MSCs Positive Antibody Cocktail159

MSCs positive cocktail	Isotype positive cocktail	Fluorochrome	Staining solution dilution in 1x PBS
CD90	Mouse IgG1, κ	FITC	5 to 100
CD105	Mouse IgG1, κ	PerCP-Cy5. 5	
CD73	Mouse IgG1, κ	APC	

Table 2. MSCs Positive Antibody Cocktail

MSCs negative cocktail	Isotype negative cocktail	Fluorochrome	Staining solution dilution in 1x PBS
CD34	Mouse IgG1, κ PE	PE	5 to 100
CD11b			
CD19			
CD45			
HLA-DR			

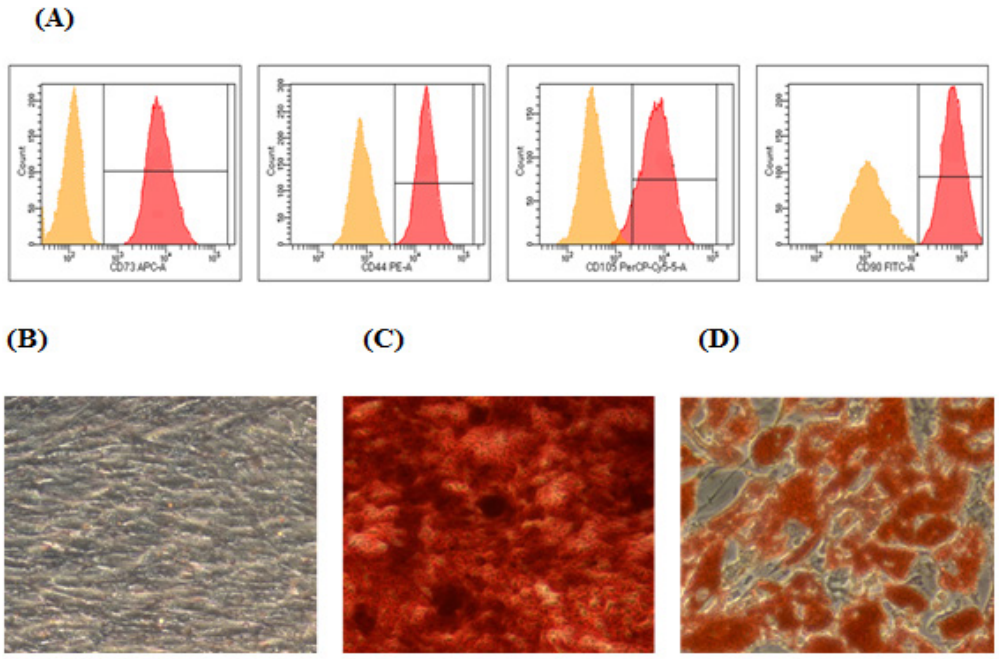

Figure 1. Characterization of AT-MSCs. (A) FACS analysis of MSCs classical markers in AT-MSCs samples represented in an overlay plots between the isotype control (orange peak) and the actual marker expression (red peak). Isotype controls were used to set the gate. Light microscopy images of adipogenic and osteogenic differentiation of AT-MSCs. (B) MSCs cultured in complete alpha-MEM. (C) Adipogenic differentiation visualized by oil red staining showing internal oil droplets generated in adipocytes. (D) Osteogenic differentiation visualized by alizarin red staining showing mineral deposit generated by osteocytes.

Table 3. CSCs Identification Antibodies

CSCs markers	Isotype control	Labeling fluorochromes	Dilution in BSA staining buffer
CD105	----------	PerCP-Cy5. 5	2 to 100
CD44	Mouse IgG2b, k	PE	2 to 100
CD24	Mouse IgG2a, k	Alexa Fluor 647	1 to 100
CD133	Mouse IgG2a, k	Brilliant violet 421	1 to 100
EpCAM/CD326	Mouse IgG2a, k	PE/Cyanine7	1 to 100

structure. The number of MSCs inoculated per well determined the size of the generated spheroid (Figure 3A, 3B, 3C, 3D, and 3E). On the other hand, colo205 cells did not form spheroids even after 5 days of culture (Figure 3F). Furthermore, the direct interaction of MSCs and cancer cells was tested in ultra-low adherent culture flasks to detect the effect of MSCs on the spheroid formation ability of colo205 cells. The coculture was conducted in a larger surface area (24 well plate and T75 flask) to monitor the natural interaction between cells without the

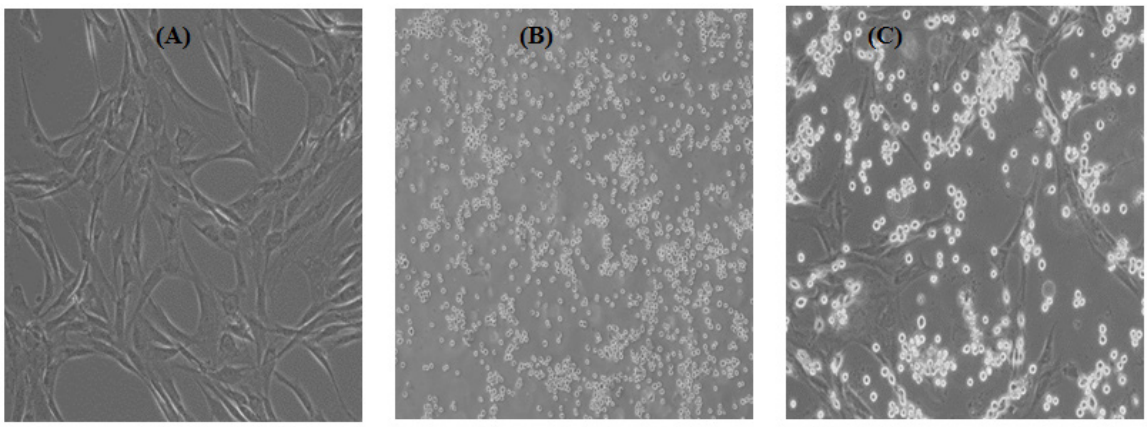

Figure 2. Light Microscopy Images of Cells after 72 hours of Coculture in Adherent Cell Culture Plate. (A) MSCs monoculture in a seeding density of 40,000 cells per well. (B) Colo205 cells monoculture in a seeding density of 40,000 cells per well. (C) Coculture of MSCs and colo205 in a ratio of 1:3 seeding density of 40,000 MSCs and 120,000 colo205 cells per well. MSCs forming a feeder layer that supports colo205 cells growth.

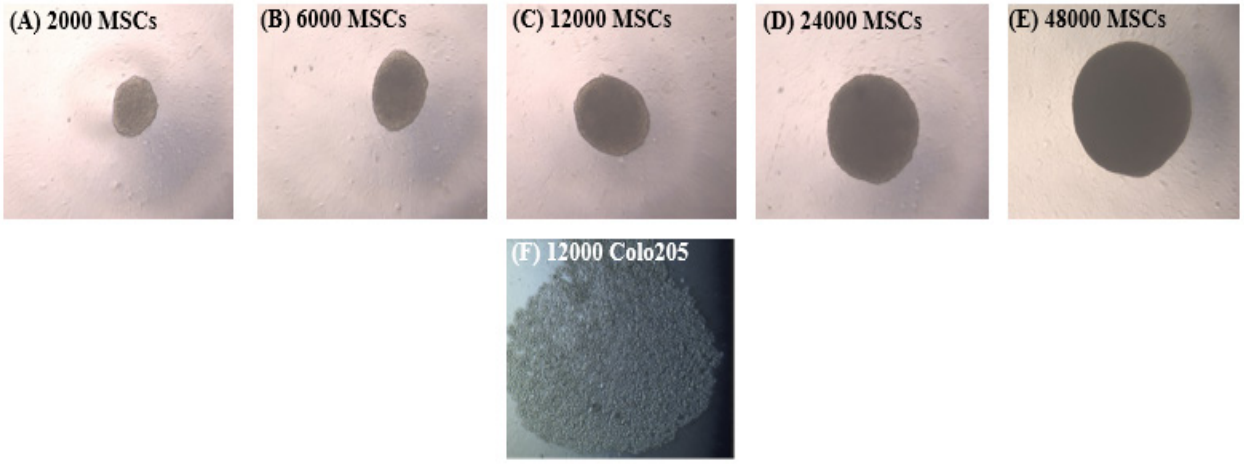

Figure 3. Spheroid Formation Aability of AT-MSCs and Colo205 Cells. MSCs spheroids established from (A) 2,000, (B) 6,000, (C) 12,000, (D) 24,000 (E) and 48,000 cells/well in ULA 96-well plate with U-bottom after 72 hours of cell inoculation. (F) 12000 Colo205 cells did not form spheroids after 72 hours of culture in ULA 96-well plate with U-bottom.

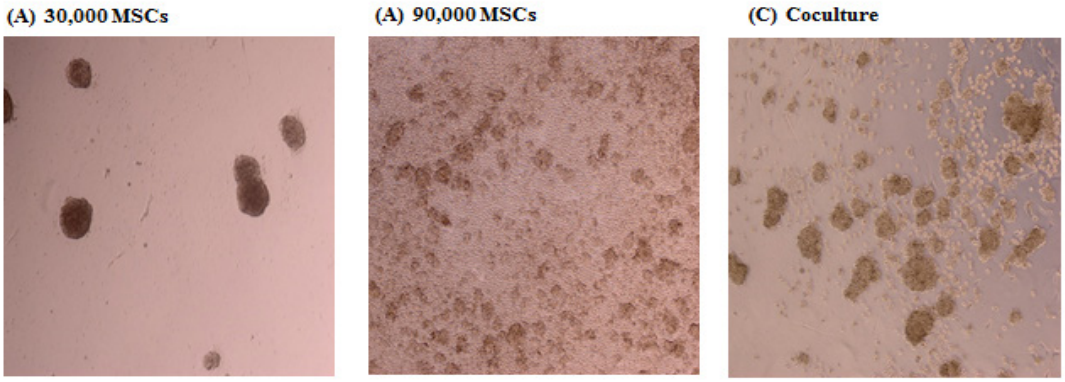

Figure 4. Colo205 and MSCs Spheroids Formation in 24 ULA-24 Well Plate. (A) MSCs monolculture at a seeding density of 30,000 cells per well. (B) Colo205 monoculture at a seeding density of 90,000 cells per well. (C) 90,000 colo205 cells cocultured with 30,000 MSCs in a single well.

reinforcement induced by the small surface area of the 96-well plate when 40,000 of MSCs were inoculated per well, they formed multiple spheroids from different sizes that are tight and intact (Figure 4A). On the other hand, when 120,000 colo205 cells were inoculated per well they formed aggregates that are fragile and dissociate with pipetting (Figure 4B). The coculture between the

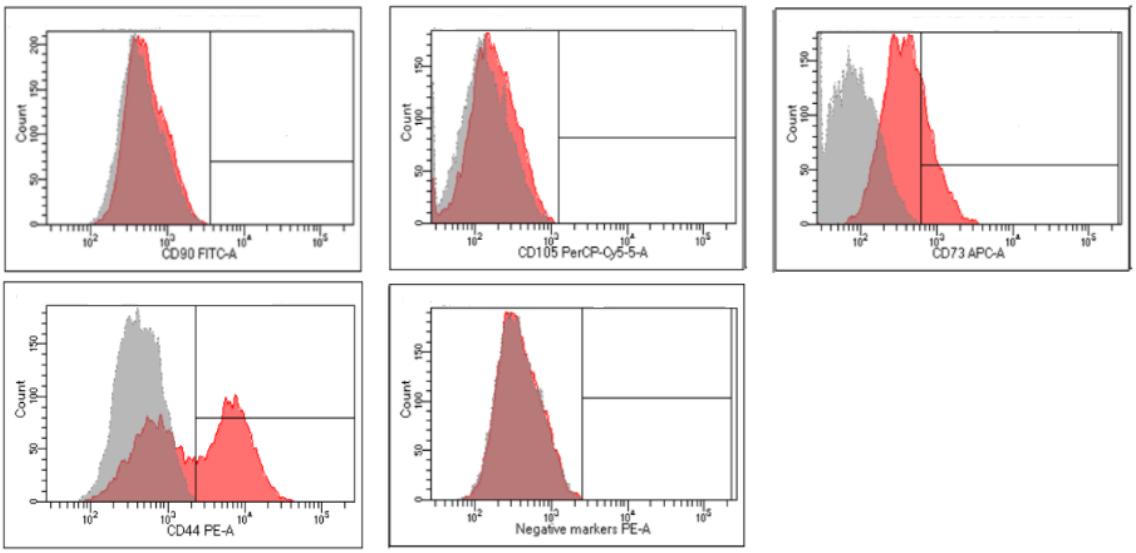

Figure 5. MSCs Classical Markers Expression in colo205 Cells. The red peak represents the actual marker expression, and the grey peak presents the isotype control.

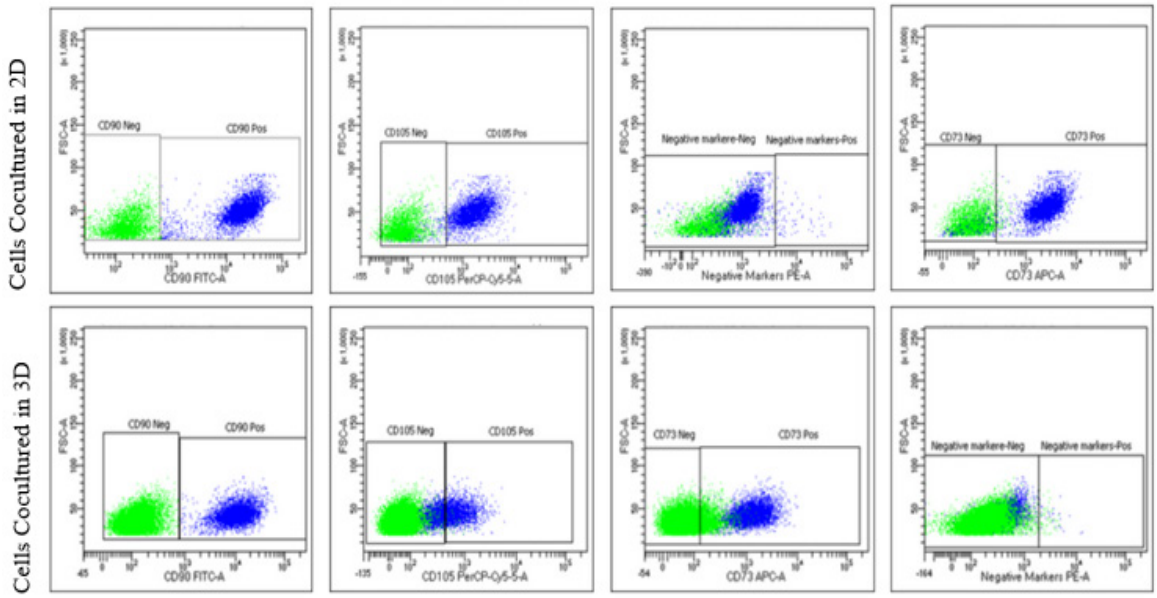

Figure 6. Expression of MSCs Classical Markers in MSCs and colo205 cells after Coculture for 72 hours. MSCs cocultured with colo205 cells in 2D culture system (upper row). MSCs cocultured with colo205 cells in 3D cell culture system (lower row). The blue population represents cells positive for CD90 expression, while the green population represents negative cells for CD90 expression.

two types of cells generated spheroids that are intact and hard to dissociate (Figure 4C).

Distinct Expression of MSCs Classical Cells in Colo205 Cells

The level of MSCs positive markers expression was tested in colo205 to define surface markers that distinguish them from MSCs after the physical direct coculture. Colo205 cells showed negative expression of CD90 and hematopoietic stem cells markers. A slightly positive expression of CD105, and a partially positive expression of CD73 and CD44 (Figure 5). However, the level of CD73 and CD44 expression in colo205 cells was lower than their expression in MSCs (Figure 6). Therefore, MSCs and colo205 cells were able to be distinguished from each other based on their level of MSCs classical markers expression MSCs in the generated tumor spheroids had a reduced level of CD105 expression (Figure 7).

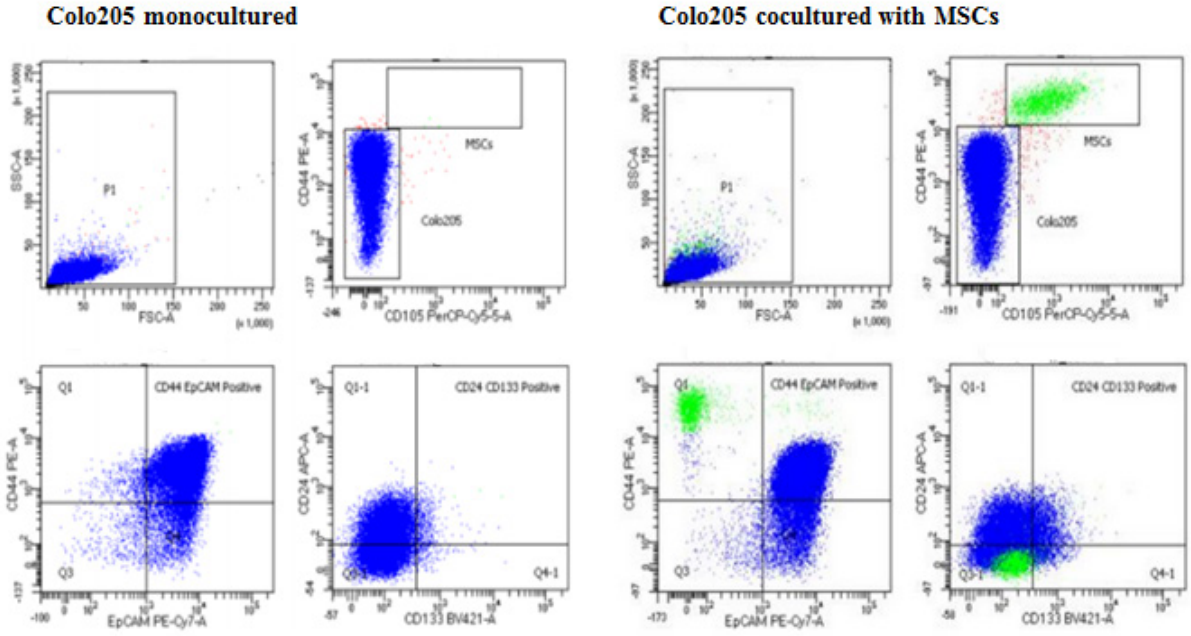

Figure 7. FACS Analysis for the Detection of CSCs in colo205 after Direct Coculture with MSCs. MSCs are Distinguished from colo205 based on Their Positive Expression of CD105 and Higher Expression of CD44. The quadrants were set using isotype controls, and the negative expression of MSCs. MSCs and colo205 are shown in green and blue colors, respectively.

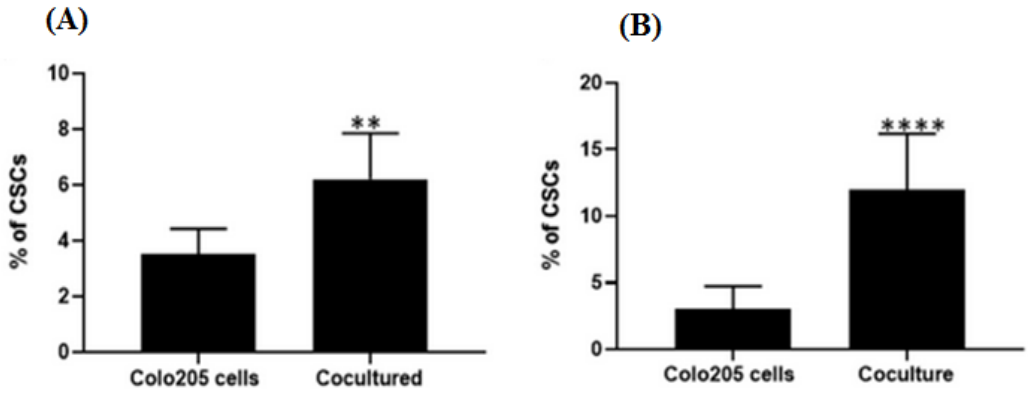

Figure 8. CSCs Induced in colo205 after Coculture with MSCs. The percentage of CSCs in colo205 co-culture with MSCs was compared to colo205 cultured alone. Each bar represents the mean of the percentage of positive cells for CSCs markers ±SEM. (A) Coculture in adherent plate significantly increased the percentage of CSCs in colo205, n = 6, **P=0.0054. (B) Coculture in ULA plate significantly increased the percentage of CSCs in colo205, n=10, ****P=0.0001.

AT-MSCs Induces the Stemness in Colo205 Cells

The effect of MSCs on the generation of CSCs in colorectal cancer was investigated. The expression of CSCs surface proteins including CD44, CD24, EpCAM and CD133 was quantified in colo205 after being co-cultured with MSCs for 72 hours in 2D and 3D cell culture. Colo205 was distinguished from MSCs in the FACS analysis based on the differences in the expression of CD44 and CD105 (Figure 7). The percentage of CSCs was determined from the quadrant in the dot plots. Furthermore, the MFI of Horizon Brilliant Violet 421 (BV421) channel was used to quantify the expression of CD133 in colo205 population. The results indicated a significant difference in the percentage of CSCs in colo205 co-cultured with MSCs (Figure 8). The observed increase in the percentage of CSCs was explained by the increased level of CD133 expression in colo205 (Figure 9).

Intracellular ROS in MSCs and Colo205 After Coculture

The effect of the direct interaction between MSCs and colo205 cells on their level of intracellular ROS was examined. DCFDA dye was used to quantify the activity of reactive oxygen species within the cells. Cells stained positively for the DCFDA dye were consideredto be ROS positive cells which were later distinguished into MSCs and colo205 cells based on their level of CD44 expression. The relative intracellular ROS concentration of MSCs and colo205 cells was detected in the FL-1 channel and measured by the MFI of that channel (Figure 10). The level of ROS in MSCs was observed to be higher than in colo205 cells. Moreover, MSCs cultured in ULA Culture system exhibit a lower level of ROS, while it was increased in colo205 cells. The direct interaction of MSCs with colo205 cells for 72 hours in standard culture condition, in both adherent and ULA culture techniques system significantly reduced the level of ROS in MSCs (Figure 11).

Discussion

Despite the fact that they originate for the same parent cells colo205 cells grow simultaneously into adherent and floating cells in adherent culture. This heterogeneity is attributed to the expression of E-cadherin and beta-

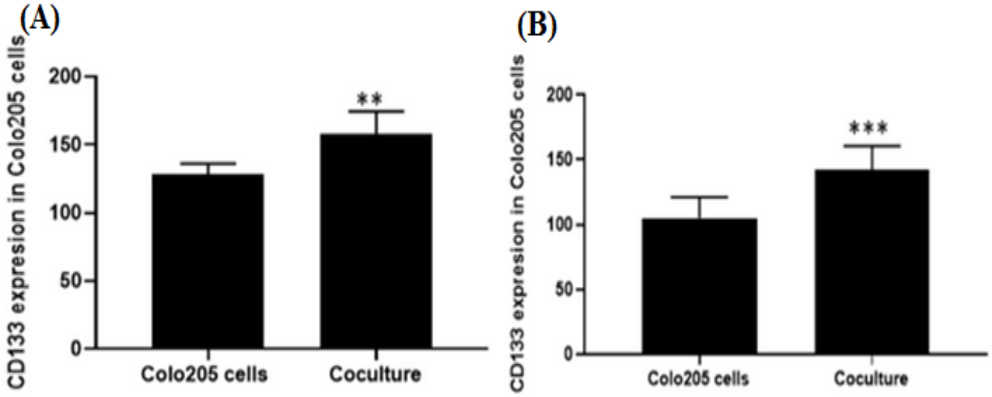

Figure 9. CD133 Expression in Colo205 after Coculture with MSCs. The MFI of the Horizon Brilliant Violet 421 (BV421) channel of colo205 co-cultured with MSCs was compared to colo205 cultured alone. Each bar represents the mean of MFI ± SEM. (A) Coculture in adherent plate significantly induced the expression of CD133 in colo205, n = 6, **P=0.0033. (B) Coculture in ULA plate significantly induced the expression of CD133 in colo205, n=10, ***P=0.0001.

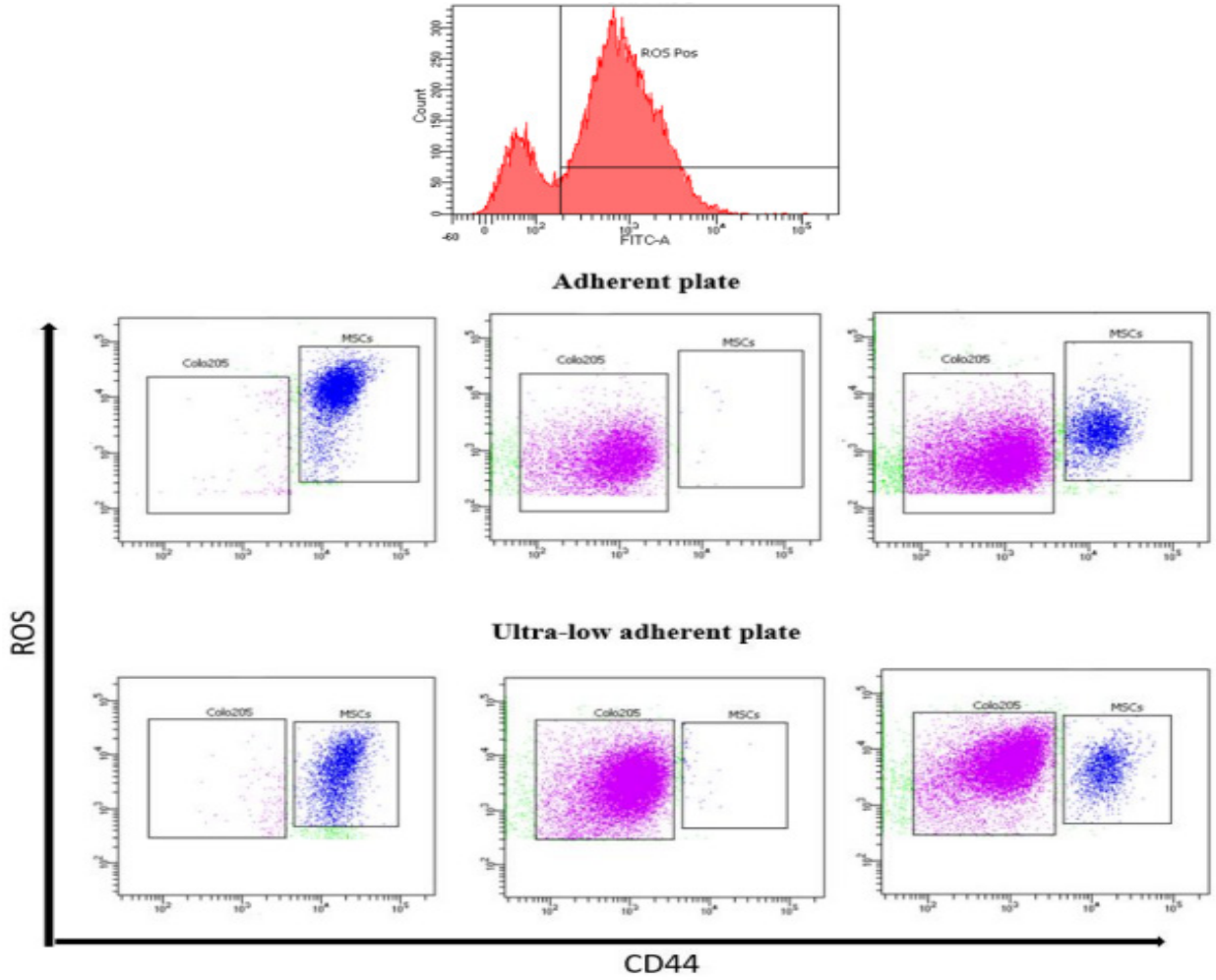

Figure 10. FACS Analysis for the Detection of Intracellular ROS in MSCs and colo205 after Coculture for 72 hours. DCFDA dye diffusion into cells and its oxidation by the reactive oxygen species was determined using unstained cells to set the gate observed in the histogram. Cells stained positively were divided into two populations based on their level of CD44 expression. Cells with lower CD44 expression represent colo205 cells (purple population), while cells with higher CD44 expression represent MSCs (blue population).

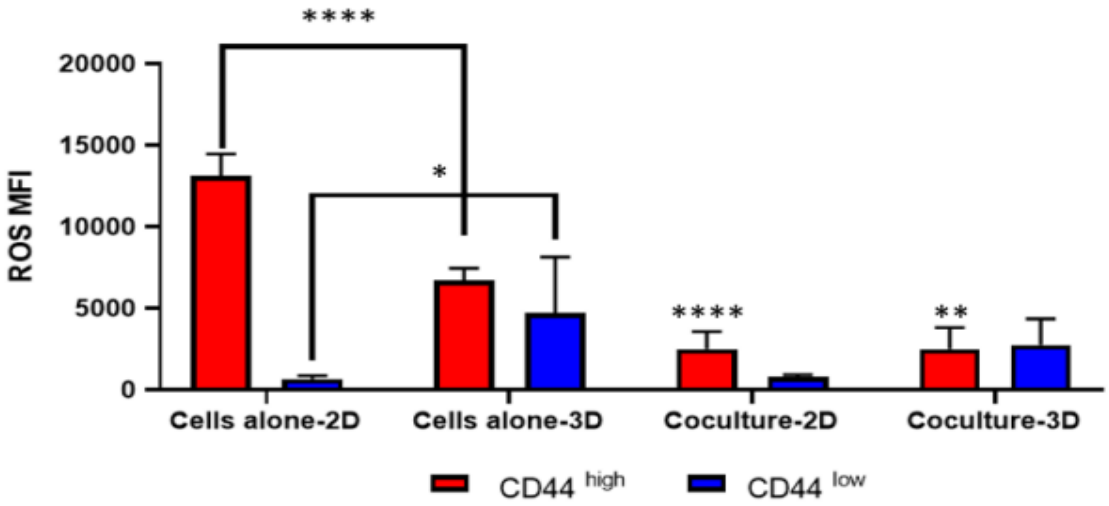

Figure 11. Changes in Intracellular ROS Levels after 72 hours of Coculture. ROS levels were measured using the MFI of the FL-1 channel. Each bar represents the mean of the MFI of each cell type ± SEM. The culture of MSCs in ULA plates significantly reduced their level of intracellular ROS, ****P<0.0001. The culture of colo205 cells significantly increased their levels of ROS, *P=0.0156. MSCs cocultured in adherent plate had a significantly reduced level of ROS, n=6, ****P<0.0001. MSCs co-cultured in ULA plate had a significantly reduced level of ROS, n=7, **P=0.0043.

catenin level of expression in where Colo205 cells with adherent state show a higher level of E-cadherin expression, while floating cells express a higher level of phosphorylated beta-catenin (Geng at al., 2014). In our study, cells were cultured in alpha-MEM supplemented with human platelets lysate using two method of cell culture; adherent and ULA cell culture plates. In adherent plate, the coculture shows how colo205 cells interact with MSCs when they are in a physically direct contact. The heterogeneity of colo205 cells was maintained where floating and adherent cells were found. However, in this case the adherent cells were attached to MSCs instead of the surface of the culture plate. Multiple cancer cells were seen attached to a single MSC which gives an indication that MSCs provide a structure for cancer cells to grow on. A strong attachment between colo205 cells and MSCs was observed which can be explained through the formation of nanotubes or gap junctions or by the two phenomena; trogocytosis and cells fusion between MSCs and tumor cells. The conducted coculture in adherent cell culture system, indicates that MSCs work as a live feeder layer consisting of proliferating cells that provide adhesion molecules and ECM component for colorectal carcinoma cells to adhere and grow this was also highlighted by other studies (Geng et al., 2014; Havasi et al., 2013). Unlike MSCs, when colo205 cells were inoculated at a low seeding density in 96-well ULA plate for 72 hours they did not form spheroids; colo205 cells were inoculated at a low seeding density to prevent the formation of a large aggregate that would mask the well. The culture of colo205 cells in plates with a larger surface area and a high seeding density led to the formation of aggregates that are fragile and dissociated easily with pipetting, these aggregate was not observed in culture when colo205 cells were inoculated 10 times lower the seeding density.

Cancer spheroids can be generated in the ultra-low adherent plate using media that is free of serum supplied with growth factors, or serum supplemented media. Serum-free media aims for CSCs enrichment. In serum-supplemented media, the formation of round shaped structure is targeted to create a 3D model in where cells of a certain tumor type are closely attached to each other. Various colorectal cancer cell lines showed the ability to generate spheroids when cultured in ultra-low adherent plate in serum-free media supplemented with growth factors. Differences in spheroids shape, size, and formation ability between cancer cells lines were observed (Sargenti et al., 2020; Hoffmann et al., 2015). Several studies reported that Colo205 cells form a loose aggregate in 3D culture, this was associated with the low cell to cell adhesion properties and the increased ability of cells to migrate and invade new sites (Stadler et al., 2018). The expression of the classical markers of MSCs were observed to define a reliable differential marker to distinguish between MSCs and colo205 cells after their direct coculture. Colo205 cells are of epithelial origin therefore they lack the expression of MSCs classical markers or exhibit a lower level of expression in comparison to MSCs. After the direct coculture, MSCs were distinguished from colo205 cells based on their higher expression of CD90, CD73, CD44 and CD105. It was also observed that colo205 cells are divided into two subpopulations based on their level of CD44. By comparing the relative expression of MSCs and colo205 of CD44, it was observed that MSCs exhibit a higher expression of CD44.

AT-MSCs show a reduced level of CD105 expression after the coculture with colo205 in ULA conditions, this was not observed in MSCs co-cultured in the adherent plate. The variation in the level of CD105 expression as a result of the culture technique was reported in other study in where the expression of CD105 in MSCs spheroids using ultra-low attachment plate decreased (Zhang et al., 2015; Krylova et al., 2015). This variation in the level of CD105 in MSCs was not related to the expression of other classical markers. Our results indicate that CD105 is not the most reliable marker to distinguish MSCs from other cells with negative expression of CD105, which was also reported by other studies. Its expression varies between MSCs from different tissue origins; bone marrow-MSCs were shown to entirely express CD105 while adipose tissue, umbilical cord, and amniotic fluid MSCs were partially positive for CD105 (Wang et al., 2018). A study showed that the level of CD105 in freshly isolated MSCs from adipose tissue is low and increased during culture passages (Mark et al., 2013). CD105 expression is also affected by the culture condition and culture duration in which its level was reduced after the culture in serum-free media and increased during long-term culture (Wang et al., 2020). Another study reported that prolonged MSCs culture in serum-containing media reduced the level of CD105 (Krylova et al., 2015).

The altered expression of CD105 on the surface of MSCs must have an impact on their response to the TGF-beta being a component of the TGF-beta receptor. MSCs might reduce their production of TGF-beta through its autocrine signaling loop which could be the reason behind the low immune-suppressive capacity of CD105 positive MSCs in comparison to CD105 negative MSCs that has been reported in several studies (Anderson et al., 2013; Pham et al., 2019). CD105 was shown to be a biomarker to indicate the stage of MSCs differentiation but not to predict the multi-lineage differentiation potential of MSCs. Despite the fact that CD105 levels are reduced when MSCs differentiate into different types of cells, there is no correlation between the capacity of MSCs differentiation and level of expression. These studies highlight the regulatory role of CD105 in MSCs differentiation (Jin et al., 2009; Cleary et al., 2016).

The physically direct coculture between AT-MSCs and colo205 cells for 72 hours in 2D and 3D increased the percentage of CD44+, CD24+, EpCAM+, CD133+, cells; these surface proteins are considered biomarkers for the identification of CSCs in colorectal cancer (Zhou et al., 206).The level of expression of each marker was investigated to reveal that the observed increase in the percent of CSCs attributes to the upregulation of CD133 in colo205 cells. In colo205 cells, CD133 was described as “the only reliable marker for the isolation and characterization of CSCs” (Vincent et al., 2014).

CD133+ population in colo205 adenocarcinoma cells had several properties of CSCs including the resistance to chemotherapy, spheroid formation, elevated level of ALDH1 expression, and tumorigenicity in vivo. Moreover, these cells had distinct metabolic profiling comparing to their negative counterpart. The obtained results from this study indicate the role of MSCs in generating of CSCs in colo205 cells. In fact, CD133 is the most known biomarkers for the isolation of CSCs from various types of cancer. The expression of CD133 on the cell surface of colorectal cancer cells was associated with their epithelial-to-mesenchymal transition and increased expression of n-cadherin and vimentin which explains their high migratory ability (Okada et al., 2021).

Cells that undergo aerobic metabolism are affected by high oxygen concentration as it triggers the formation of oxidative stress which is defined as an imbalance between ROS and antioxidants. A high concentration of ROS can cause serious damage to the cells including DNA mutation, cell senescence, and/or death through the oxidation of DNA, proteins, and lipids. In their niche, MScs are exposed to low oxygen tension that is estimated to be in the range of 1-8%. In vitro, MSCs are cultured in standard conditions with higher oxygen tension that is equal to 20%. Studies show that hypoxic condition enhances the stemness of MScs and reduce their differentiation potential (Ali et al., 2016; Ejtehadifar et al., 2015).

Decreased osteogenic and chondrogenic differentiation potential was reported in adipose tissue- Derived MSCs cultured in hypoxic conditions. Moreover, hypoxic conditions were shown to lower the proliferation rate of adipose tissue-derive MSCs. This gives a hint of the importance and necessity of the hypoxic conditions presented in the niche of MSCs, it also can explain the low survival rate of implanted MSCs (Ali et al., 2016). Several factors contribute to the formation of reactive oxygen species in tumor cells including their increased metabolic activity, enzyme activity, and receptor signaling. Tumor cells also express an increased level of antioxidants to balance their high levels of ROS. Increased intracellular ROS in tumor cells was correlated to their epithelial-mesenchymal transition, migration, and increased invasion potential. In this study, it was observed that MSCs cultured in monolayer had a higher level of ROS compared to cells cultured in ULA plates. MSCs had a higher level of ROS compared to colo205 cells when cells were cultured separately. After 72 hours of co-culture, the level of ROS was reduced dramatically in MSCs, while a slight increase in the level of ROS was observed in colo205 cells, due probably to the reduced diffusion of oxygen to the cells. Moreover, the study showed that MSCs exhibit a higher level of ROS comparing to colo205 cells, because increased antioxidants in tumor cells in order to compensate for their high production of ROS. The production of ROS in MSCs was significantly reduced in MSCs after coculture with cancer cells for 72 hours, this reduction was observed in MSCs cocultured colo205 cells in adherent in 2D and ULA plates in 3D.

Our results indicates that AT-MSCs provide physical support for the growth of colorectal carcinoma cells and spheroids formation, along with enhancing their stemness. On the other hand, the presence of MSCs in a direct physical contact with colorectal carcinoma cells triggers their CAFs MSCs molecular signature in MSCs, and reduced their levels of ROS. These results describe the complementary relationship between MSCs and colon cancer cells in the TME of colorectal cancer.

In conclusion, through the direct interaction a symbiotic relationship between AT-MSCs and colo205 was revealed. Despite the promising results provided by different reports, more research has to be oriented toward the interaction mechanism of MSCs and cancer cells in order to evaluate MSCs in cellular therapy.

Author Contribution Statement

Amjad Mahasneh: Conceptualization; Investigation; Supervision; Project administration; critical review of the manuscript. Nour Sharar: Methodology before Data collection so it reads, Methodology, Data collection. Djeda Belharazem, Nidaa Ababneh, and Abdalla Awidi; Investigation; supervision, critical review of the manuscript.

Acknowledgments

We would like to thank Dr. Ahmad Telfah and Dr. Hanan Jafar for their valuable thoughts and comments throughout the course of the work. Also, we would like to thank the Cell Therapy Center for hosting Nour and providing necessary equipment.

Funding Statement

This work was supported by the Deanship of Research at Jordan University of Science and Technology, Jordan (Grant number 538/2020).

Scientific Approval

This paper is part of an approved Master thesis for Nour Sharar who was a graduate student and obtained her degree in 2021.

Conflicts of interest

The authors declare that they have no conflict of interest

References

Abuarqoub DA, Aslam N, Barham RB, et al (2019). The effect of platelet lysate in culture of PDLSCs: an in vitro comparative study. *Peer J*, **7**, e7465.

Abuarqoub D, Awidi A, Abuharfeil N (2015). Comparison of osteo/odontogenic differentiation of human adult dental pulp stem cells and stem cells from apical papilla in the presence of platelet lysate. *Arch Oral Biol*, **60**, 1545-53.

Ali NM, Boo L, Yeap SK, et al (2016). Probable impact of age and hypoxia on proliferation and microRNA expression profile of bone marrow-derived human mesenchymal stem cells. *Peer J*, **4**, e1536.

Alonso-goulart V, Braga L, Angélico C (2017). Mesenchymal stem cells from human adipose tissue and bone repair: a literature review. *Biotechnol Res Innov*, **2**, 74-80.

Anderson P, Carrillo-Gálvez AB, García-Pérez A, Cobo M, Martín F (2013). CD105 (endoglin)-negative murine mesenchymal stromal cells define a new multipotent subpopulation with distinct differentiation and immunomodulatory capacities. *PLoS One*, **8**, e76979.

Berebichez-Fridman R, Montero-Olvera PR (2018). Sources and clinical applications of mesenchymal stem cells state-of-the-art review. *Sultan Qaboos Univ Med J*, **18**, 264–77.

Chen R, Huang L, Hu K (2020). Natural products remodel cancer-associated fibroblasts in desmoplastic tumors. *Acta Pharm Sinic B*, **10**, 2140-55.

Cleary MA, Narcisi R, Focke K, et al (2016). Expression of CD105 on expanded mesenchymal stem cells does not predict their chondrogenic potential. *Osteoarthritis Cartilage*, **24**, 868-72.

Cuiffo BG, Karnoub AE (2012). Mesenchymal stem cells in tumor development: emerging roles and concepts. *Cell Adhes Migr*, **6**, 220–30.

Dominici ML, Le Blanc K, Mueller I, et al (2006). Minimal criteria for defining multipotent mesenchymal stromal cells. The International Society for Cellular Therapy position statement. *Cytotherapy*, **8**, 315-7.

Eggenhofer E, Luk F, Dahlke MH, Hoogduijn MJ (2014). The life and fate of mesenchymal stem cells. *Front Immunol*, 5, 148.

Ejtehadifar M, Shamsasenjan K, Movassaghpour A, et al (2015). The effect of hypoxia on mesenchymal stem cell biology. *Adv Pharm Bull*, **5**, 141-9.

Eser S, Chang J, Charalambous H, et al (2018). Incidence patterns of colorectal cancers in four countries of the middle east cancer consortium (Cyprus, Jordan, Israel, And Izmir, Turkey) compared with those in the united states surveillance, epidemiology, and end results program. *Turk J Gastroenterol*, **29**, 36.

Geng Y, Chandrasekaran S, Agastin S, Li J, King MR (2014). Dynamic switch between two adhesion phenotypes in colorectal cancer cells. *Cell Mol Bioeng*, **7**, 35-44.

Havasi P, Nabioni M, Soleimani M, Bakhshandeh B, Parivar K (2013). Mesenchymal stem cells as an appropriate feeder layer for prolonged in vitro culture of human induced pluripotent stem cells. *Mol Biol Rep*, **40**, 3023-31.

Hoffmann OI, Ilmberger C, Magosch S, et al (2015). Impact of the spheroid model complexity on drug response. *J Biotechnol*, **205**, 14-23.

Jin HJ, Park SK, Oh W, et al (2009). Down-regulation of CD105 is associated with multi-lineage differentiation in human umbilical cord blood-derived mesenchymal stem cells. *Biochem Biophys Res Commun*, **381**, 676-81.

Joyce N, Annett G, Wirthlin L, et al (2010). Mesenchymal stem cells for the treatment of neurodegenerative disease. *Regen Med*, **5**, 933-46.

Krylova TA, Musorina AS, Zenin VV, Poljanskaya GG (2015). Cellular spheroids obtained from mesenchymal stem cells derived from bone marrow and limb muscle of early human embryo. *Cell Tissue Biol*, **9**, 431-40.

Kucerova L, Altanerova V, Matuskova M, Tyciakova S, Altaner C (2007). Adipose tissue–derived human mesenchymal stem cells mediated prodrug cancer gene therapy. *Cancer Res*, **67**, 6304-13.

Lukomska B, Stanaszek L, Zuba-Surma E, et al (2019). Challenges and controversies in human mesenchymal stem cell therapy. *Stem Cells Int*, **2**, 1-10.

Mark P, Kleinsorge M, Gaebel R, et al (2013). Human mesenchymal stem cells display reduced expression of CD105 after culture in serum-free medium. *Stem Cells Int*, **2013**, 698076.

Mohamed-Ahmed S, Fristad I, Lie SA, et al (2018). Adipose-derived and bone marrow mesenchymal stem cells: a donor-matched comparison. *Stem Cell Res Ther*, **9**, 1-5.

Murphy JM, Dixon K, Beck S, et al (2002). Reduced chondrogenic and adipogenic activity of mesenchymal stem cells from patients with advanced osteoarthritis. *Arthritis Rheum*, **46**, 704-13.

Okada M, Kawai K, Sonoda H, et al (2021). Epithelial-mesenchymal transition and metastatic ability of CD133+ colorectal cancer stem-like cells under hypoxia. *Oncol Lett*, **21**, 19.

Pham LH, Vu NB, Van Pham P (2019). The subpopulation of CD105 negative mesenchymal stem cells show strong immunomodulation capacity compared to CD105 positive mesenchymal stem cells. *Biomed Res Ther*, **6**, 3131-40.

Powell DW, Adegboyega PA, Di Mari JF, Mifflin RC (2005). Epithelial cells and their neighbors I. Role of intestinal myofibroblasts in development, repair, and cancer. *Am J Physiol-Gastr L*, **289**, G2-7.

Rawla P, Sunkara T, Barsouk A (2019). Epidemiology of colorectal cancer: incidence, mortality, survival, and risk factors. *Prz Gastroenterol*, **14**, 89.

Sargenti A, Musmeci F, Bacchi F, et al (2020). Physical Characterization of Colorectal Cancer Spheroids and Evaluation of NK Cell In fi ltration Through a Flow-Based Analysis. *Front Immunol*, **11**, 564887.

Schu S, Nosov M, O'Flynn L, et al (2012). Immunogenicity of allogeneic mesenchymal stem cells. *J Cell Mol Med*, **16**, 2094-103.

Stadler M, Scherzer M, Walter S, et al (2018). Exclusion from spheroid formation identifies loss of essential cell-cell adhesion molecules in colon cancer cells. *Sci Rep*, **8**, 1-6.

Tao L, Huang G, Song H, Chen Y, Chen L (2017). Cancer associated fibroblasts: An essential role in the tumor microenvironment. *Oncol Lett*, **14**, 2611-20.

Ullah M, Liu DD, Thakor AS (2019). Mesenchymal stromal cell homing: mechanisms and strategies for improvement. *Iscience*, **15**, 421-38.

Vincent Z, Urakami K, Maruyama K, Yamaguchi K, Kusuhara M (2014). CD133-positive cancer stem cells from Colo205 human colon adenocarcinoma cell line show resistance to chemotherapy and display a specific metabolomic profile. *Genes Cancer*, **5**, 250.

Wang D, Liu N, Xie Y, et al (2020). Different culture method changing CD105 expression in amniotic fluid MSCs without affecting differentiation ability or immune function. *J Cell Mol Med*, **24**, 4212-22.

Wang S, Miao Z, Yang Q, Wang Y, Zhang J (2018). The dynamic roles of mesenchymal stem cells in colon cancer. *Can J Gastroenterol Hepatol*, **2018**, 7628763.

Zhang J, Huang X, Wang H, et al (2015). The challenges and promises of allogeneic mesenchymal stem cells for use as a cell-based therapy. *Stem Cell Res Ther*, **6**, 1-7.

Zhou Y, Huang Y, Cao X, et al (2016). WNT2 promotes cervical carcinoma metastasis and induction of epithelial-mesenchymal transition. *PLoS One*, **11**, e0160414.